

Chapter 3

Attitude Control with Thrusters

3.1 Fast Versus Slow Attitude Control

If the desired attitude control bandwidth is large compared to orbit rate n , then gravity or magnetic torques are small compared to the required control torques. Hence, they may be treated as disturbance torques, using a free space model of the spacecraft dynamics. We shall call this *fast attitude control*.

If, on the other hand, the satellite mission is such that a control bandwidth comparable to the orbit rate is acceptable, then gravity or magnetic torques can be used with reaction wheels (or gimballed momentum wheels; see Chapter 6) to stabilize the satellite *without the use of thrusters*. We shall call this *slow attitude control*. The use of slow attitude control requires careful configuration design to keep disturbance torques acceptably small.

We shall not discuss slow attitude control with passive libration dampers. This type of damping was used in the early days of the space era (Ref. SY), but has been succeeded by improved methods. It is difficult to build light-weight passive dampers that will dissipate energy at the low libration frequencies.

3.2 Fast Attitude Control Using Proportional Thrusters

If the available control torques are large compared to the disturbance torques, and we wish to *stabilize* the spacecraft attitude *with respect to inertial space*, then the attitude motions about the three principal axes are nearly uncoupled, and stabilization about each principal axis may be treated separately (see Fig. 3.1).

A convenient inertial reference system in interplanetary space is the celestial sphere.

In this section, we consider the somewhat unrealistic case where *proportional thrusters* are available to produce torques about each of the three principal axes. Proportional thrusters are *not* easily achieved in practice; we treat them here for pedagogical reasons, since control logic for such thrusters is simpler than control logic for the more practical on-off thrusters, which are treated in the next section.

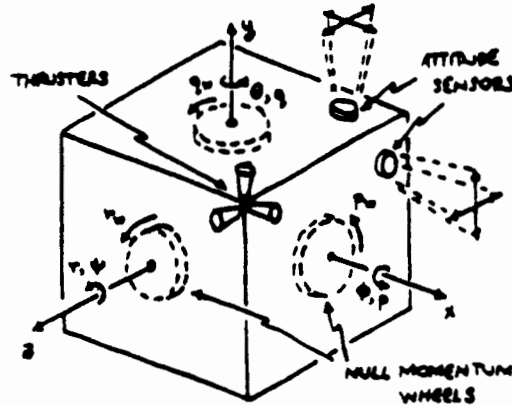


Figure 3.1: Three-Axis Attitude Control Thrusters, Wheels, and Sensors

If *both attitude and attitude-rate are sensed* (e.g., using a sun sensor, a star sensor, and three rate gyros), then stabilization about each principal axis may be obtained by feeding back a linear combination of attitude deviation and attitude-rate to the torquer. For example, about the body y -axis:

$$Q_y = -D\dot{\theta} - K\theta , \quad (3.1)$$

where

$$I_y\ddot{\theta} = Q_y , \quad (3.2)$$

Clearly, for $D > 0$, $K > 0$, the motion is stabilized.

If *only attitude is sensed* (gyros consume power, reduce reliability, and they cost and weigh more than the devices needed to implement the control logic below) then stabilization about each principal axis may be obtained by feeding back attitude deviation with *lead compensation* to the torquer. For example, about the body y - axis:

$$Q_y = -K(\theta - \xi) , \quad (3.3)$$

$$\dot{\xi} + b\xi = (b - a)\theta . \quad (3.4)$$

In *transfer function notation*, (2)-(4) become:

$$Q_y(s) = -K \frac{s + a}{s + b} \theta(s) , \quad (3.5)$$

$$\theta(s) = \frac{1}{I_y s^2} Q_y(s) . \quad (3.6)$$

Fig. 3.2 shows a block diagram of the system, including the possibility of commanding a non-zero value of θ , called θ_c .

The characteristic equation of the system (5) and (6), in Evans' form is:

$$- \frac{K}{I_y} = \frac{s^2(s + b)}{s + a} . \quad (3.7)$$

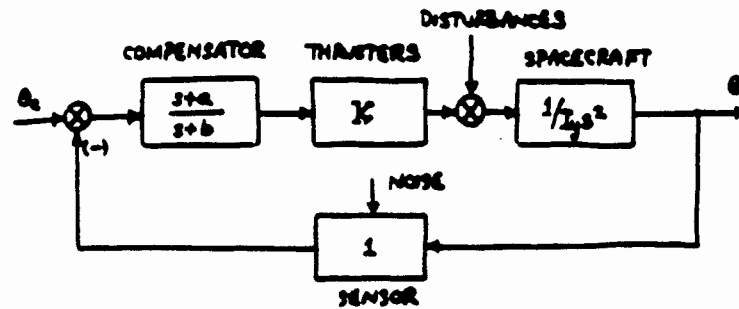


Figure 3.2: Attitude Control System with Proportional Thrusters and Attitude Sensor

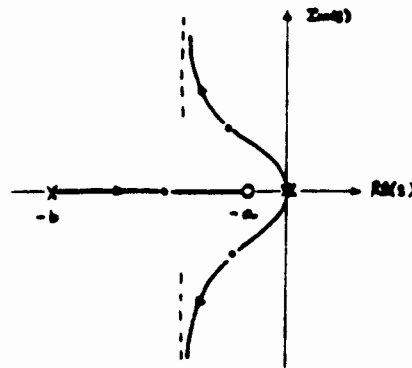


Figure 3.3: Locus of Closed-Loop Roots vs. Feedback Gain K for System of Fig. 3.2

Fig. 3.3 shows a root locus versus K for $b > a > 0$. Clearly the attitude is stabilized.

Problem 3.2.1 - Second-Order Estimator Using Attitude Angle

Show that attitude-rate q , and attitude θ , may be estimated using a noisy measurement of attitude z_y by the system

$$\begin{aligned} \dot{\hat{q}} &= \frac{Q_y}{I_y} + k_q(z_y - \hat{\theta}) , \\ \dot{\hat{\theta}} &= \hat{q} + k_\theta(z_y - \hat{\theta}) , \end{aligned}$$

where $k_q > 0, k_\theta > 0$.

Problem 3.2.2 - Second-Order Compensator Synthesis Using an Estimator

(a) If we use estimated-state feedback, i. e. modify (1) to

$$Q_y = -D\hat{q} - K\hat{\theta} ,$$

where \hat{q} and $\hat{\theta}$ are obtained with the estimator of Problem 3.2.1, show that this yields a second-order compensator, $Q_y(s)/z_y(s)$.

- (b) Choose D and K to place the poles of the regulator, (1) and (2) at $s = -\omega_o \pm \omega_o j$ and choose k_q and k_θ in Problem 3.2.1 to place the estimate-error poles at $s = -\omega_o \pm \omega_o j$.
- (c) Show that the closed-loop system has double poles at $s = -\omega_o \pm \omega_o j$.
- (d) Show that the compensator is:

$$\frac{Q_y(s)}{I_y} = -8\omega_o^3 \frac{s + \omega_o/2}{(s + 2\omega_o)^2 + (2\omega_o)^2} z_y(s) .$$

- (e) Multiply the right-hand side of the equation in (d) by k_o and sketch a root locus versus k_o of the closed-loop system with this compensator. Note for $k_o = 1$, the root locus must have double poles at $s = -\omega_o \pm \omega_o j$.

Problem 3.2.3 - First-Order Estimator Using Attitude Angle

Show that attitude-rate q , can be estimated from a relatively noise- free measurement of attitude z_y , by the system

$$\begin{aligned} \hat{q} &= q^* + \ell z_y , \\ \dot{q}^* &= -\ell \hat{q} + Q_y/I_y , \end{aligned}$$

where $\ell > 0$. Note that

$$\dot{\hat{q}} = Q_y/I_y + \ell(z_y - \hat{q}) .$$

Problem 3.2.4 - First-order Compensator Synthesis Using an Estimator

- (a) If we use $Q_y = -D\hat{q} - Kz_y$, where \hat{q} is obtained with the estimator of Problem 3.2.3, show that this yields a classical lead compensator, $Q_y(s)/z_y(s)$.
- (b) Choose D and K to place the poles of the regulator (1) and (2) at $s = -\omega_o \pm \omega_o j$, and choose ℓ in Problem 3.2.3 to place the estimate-error pole at $s = -\omega_o$.
- (c) Show that the closed-loop system has poles at $s = -\omega_o \pm \omega_o j, -\omega_o$.
- (d) Show that the compensator is

$$\frac{Q_y(s)}{I_y} = -4\omega_o^2 \frac{s + \omega_o/2}{s + 3\omega_o} z_y(s) .$$

- (e) Multiply the right-hand side of the equation in (d) by k_o , sketch a root locus versus k_o of the closed-loop system with the compensation. Note for $k_o = 1$, the root locus must pass through $s = -\omega_o \pm \omega_o j$ and $s = -\omega_o$.

3.3 Fast Attitude Control Using On-Off Thrusters

3.3.1 On-Off Thrusters

Proportional gas jets are difficult to build; they usually have a large amount of hysteresis. In addition, proportional valves need only open a small amount to produce the small torques required for control; as a result, dirt and ice particles tend to stick in the valve openings and they do not close completely. The resulting leakage causes the opposing jets to open and the gas supply dwindles rapidly! Consequently, control techniques have been developed where the valves are either completely open or completely closed ("on-off" or "bang-bang" control). Large springs may be used to hold them shut, thereby reducing leakage; the closing "bang" jars loose any ice or dirt particles.

Valves can be operated to stay open as little as a few milliseconds, and can be fired over a million times reliably, but the valves must stay open a finite length of time and therefore, there is a discrete angular velocity change with each actuation of the valve. As a result, it is not possible to get zero residual angular velocity as it is in principle with a proportional valve.

To prevent opposing jets from fighting each other, there must be a deadband in a system using on-off control. When the vehicle is in the deadband, no control action is taken. When the error signal—which is made up of vehicle attitude and attitude-rate information—exceeds the deadband, then the gas valves are appropriately modulated.

3.3.2 Bang-Bang Control (No Deadband)

A simple on-off reaction jet control scheme is obtained using a "linear switching function". If the control torque has only two values (Q_o and $-Q_o$), we can bring θ and $\dot{\theta}$ almost to zero by the control logic

$$Q = -Q_o \operatorname{sgn}(\theta + \tau \dot{\theta}) , \quad (3.8)$$

where

$$\operatorname{sgn}(x) \triangleq \begin{cases} 1 & x > 0 \\ -1 & x < 0 \end{cases} ,$$

and $\theta + \tau \dot{\theta}$ is the *switching function*, which, in this case, is a linear combination of θ and $\dot{\theta}$. A phase plane diagram of the system behaviour is shown in Fig. 3.4.

For $Q = \text{constant}$:

$$\dot{\theta} = \frac{Q}{I}(t - t_o) + \dot{\theta}_o , \quad (3.9)$$

$$\theta = \frac{1}{2} \frac{Q}{I}(t - t_o)^2 + \dot{\theta}_o(t - t_o) + \theta_o . \quad (3.10)$$

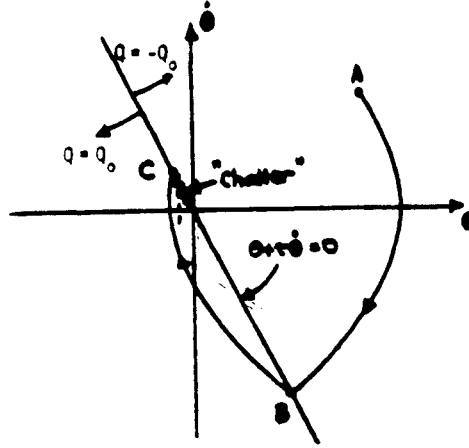


Figure 3.4: Phase Plane Path of a Bang-Bang Control System with a Linear Switching Function

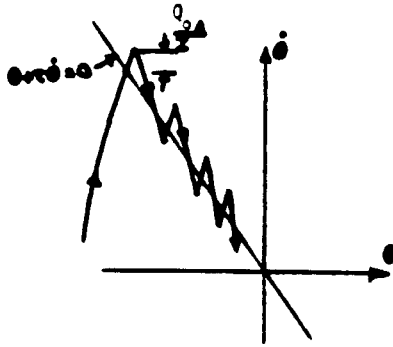


Figure 3.5: Chatter Along the Switching Line in the Phase Plane

Eliminating $t - t_0$:

$$\theta - \theta_0 = \frac{I}{2Q}(\dot{\theta} - \dot{\theta}_0)^2 + \frac{I}{Q}\dot{\theta}_0(\dot{\theta} - \dot{\theta}_0) \equiv \frac{I}{2Q}(\dot{\theta}^2 - \dot{\theta}_0^2), \quad (3.11)$$

$$\Rightarrow \dot{\theta}^2 = \frac{2Q}{I} \left(\theta - \theta_0 + \frac{I}{2Q}\dot{\theta}_0^2 \right), \quad (3.12)$$

which is a parabola in the $\theta, \dot{\theta}$ phase space. The path in the phase space is made up of parabolas until a point like C is reached where the next parabola does not occur to the right of the switching line but starts off to the left; due to the finite time (Δ) necessary to switch the jets off and on, the path actually over-shoots the switching line a small amount, and the torque reversal sends the path back across the switching line, reversal occurs, etc. giving rise to a high frequency chatter shown in Fig. 3.5.

The path essentially follows $\tau\dot{\theta} + \theta \cong 0 \Rightarrow \theta \cong \theta_c \exp(-(t - t_c)/\tau)$, so the system moves toward $\theta = \dot{\theta} = 0$.

The chatter is caused here by the time delay (Δ) in switching the jets on and off. Unfortunately, the point $\theta = \dot{\theta} = 0$ is never reached; instead a *limit cycle* around that point occurs

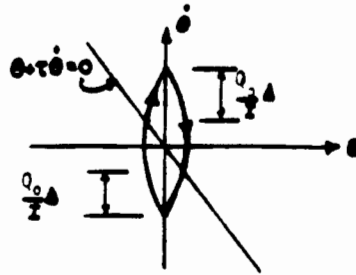


Figure 3.6: Limit Cycle Around $\theta = \dot{\theta} = 0$ A Nonlinear Oscillator

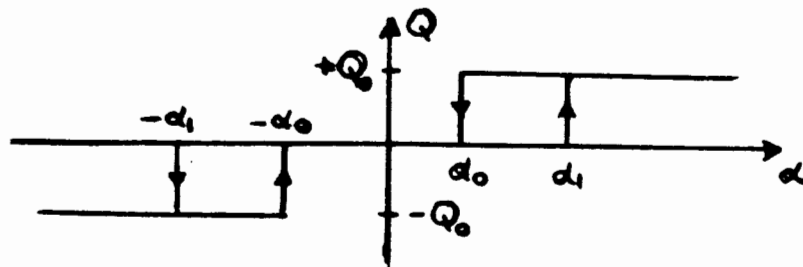


Figure 3.7: Output vs. Input with Dead Zone and Hysteresis (Schmitt Trigger)

as shown in Fig. 3.6. Obviously this wastes fuel so some other scheme with a *dead-zone* (where $Q = 0$ is used) is desired.

3.3.3 Bang-Off-Bang Control

To make effective use of a dead-zone we also use *hysteresis*; dead- zone and hysteresis are combined in a scheme called a Schmitt trigger, shown in Fig. 3.7.

It is simple to use the Schmitt trigger with a *linear switching function* as shown in Fig. 3.8.

This control system cannot bring θ and $\dot{\theta}$ to zero but at least it can bring them to acceptably small values, ending with a low frequency limit cycle which does not use as much fuel as the bang-bang scheme. It is straight forward to show that the limit cycle period and

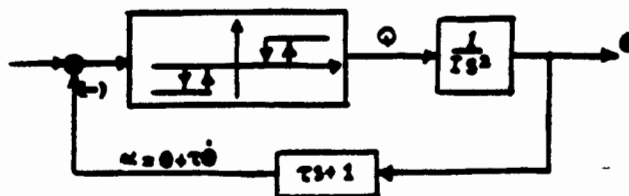


Figure 3.8: Block Diagram of Schmitt Trigger Used with a Linear Switching Function

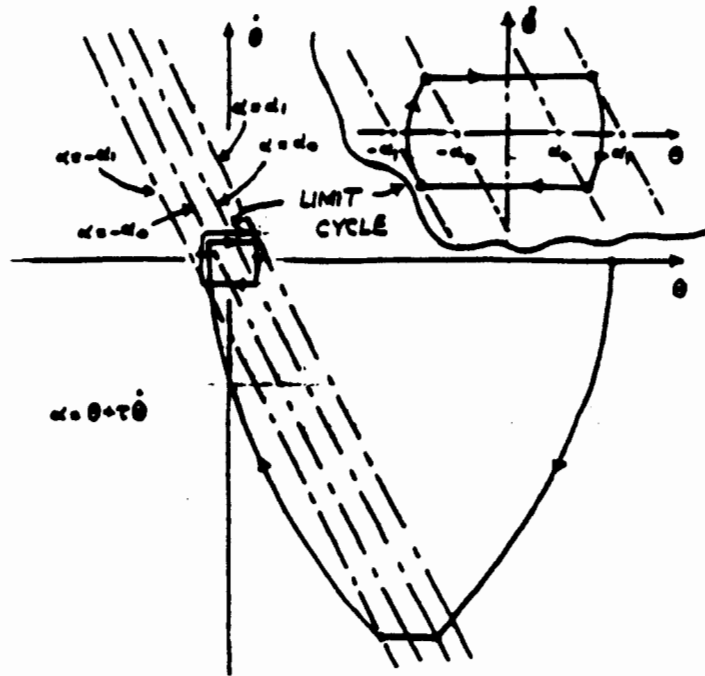


Figure 3.9: Phase Plane Path; Attitude Control Using Deadband and Hysteresis (Schmitt Trigger)

amplitude are given by (see Fig. 3.9):

$$\text{Period} = 4\tau \left(\frac{\alpha_1 + \alpha_0}{\alpha_1 - \alpha_0} + \frac{\alpha_1 - \alpha_0}{2N\tau^2} \right), \quad N \triangleq \frac{Q_0}{I}, \quad (3.13)$$

$$\text{Amplitude} = \frac{1}{2}(\alpha_1 + \alpha_0) + \frac{1}{8} \frac{(\alpha_1 - \alpha_0)^2}{N\tau^2}. \quad (3.14)$$

Problem 3.3.1 - Limit Cycle Period and Amplitude

- (a) Given the pitch dynamics

$$I\ddot{\theta} = Q,$$

and the Schmitt trigger of Fig. 3.7, verify the expressions for limit cycle period and an amplitude given in equations (5) and (6).

- (b) For $\alpha_0 = 1$ degree, $\alpha_1 = 3$ degrees, $N \equiv Q_0/I = 1/3$ degree/sec², $\tau = 5$ sec, determine the period, and amplitudes of θ and $\dot{\theta}$ in the limit cycle, and plot the limit cycle in the $(\dot{\theta}, \theta)$ plane.
- (c) Using the data in (b), calculate the response for $\theta(0) = 30^\circ$, $\dot{\theta}(0) = 0$ and plot the response in the $(\dot{\theta}, \theta)$ plane.

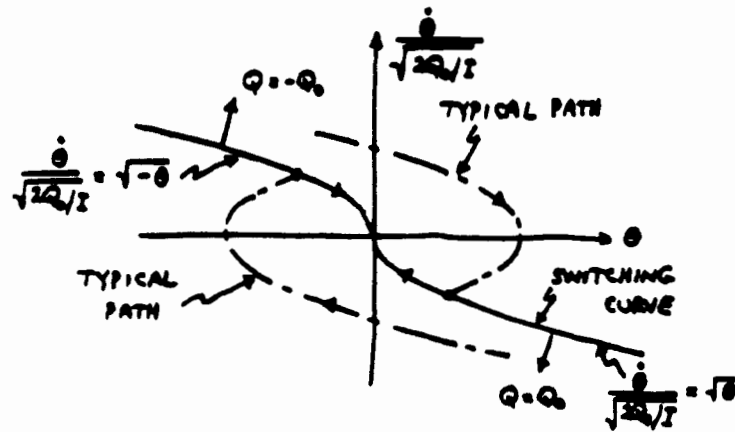


Figure 3.10: Minimum Time Bang-Bang Control of Attitude (Quadratic Switching Function)

Problem 3.3.2 - Minimum Time Bang-Bang Control of Attitude

Minimum-time control of attitude to $\theta = \dot{\theta} = 0$ using two on-off torquers (one for positive torque, one for negative torque) is achieved using the *nonlinear switching* function shown in Fig. 3.10 (see e. g. Ref. BR-1, pp. 112-113); only one switch is required.

Starting with $\theta(0) = 30^\circ$, $\dot{\theta}(0) = 0$, calculate the time (in units of $1/\sqrt{2Q_0/I}$) to $\theta = \dot{\theta} = 0$ using the linear switching function with $\frac{1}{T} = \sqrt{2Q_0/I}$, and with the minimum-time switching function.